Oscillating Bubble SHG on Surface Elastic and Surface Viscoelastic Systems: New Insights in the Dynamics of Adsorption Layers

A. Andersen, J. Oertegren, P. Koelsch, D. Wantke, and H. Motschmann*

Max-Planck-Institute of Colloids and Interfaces, Am Mühlenberg 1, 14424 Golm/Potsdam, Germany

Received: May 17, 2006; In Final Form: July 12, 2006

Surface rheology governs a great variety of interfacial phenomena such as foams or emulsions and plays a dominant role in several technological processes such as high-speed coating. Its major difference with bulk rheology resides in the high compressibility of the surface phase, which is the direct consequence of the molecular exchange between adsorbed and dissolved species. In analogy to bulk rheology, a complex surface dilational modulus, ϵ, which captures surface tension changes upon defined area changes of the surface layer, can be defined. The module ϵ is complex, and the molecular interpretation of the dissipative process that gives rise to the imaginary part of the module is subject to some controversy. In this contribution, we used the oscillating bubble technique to study the surface dilational modulus in the mid-frequency range. The dynamic state of the surface layer was monitored by a pressure sensor and by surface second-harmonic generation (SHG). The pressure sensor measures the real and imaginary part of the modulus while SHG monitors independently the surface composition under dynamic conditions. The experiment allows the assessment of the contribution of the compositional term to the surface dilational modulus ϵ. Two aqueous surfactant solutions have been characterized: a surface elastic and a surface viscoelastic solution. The elastic surface layer can be described within the framework of the extended Lucassen−van den Tempel Hansen model. The change in surface concentration is in phase with the relative area change of the surface layer, which is in strong contrast with the results obtained from the surface viscoelastic solution. Here, surface tension, area change, and surface composition are phase-shifted, providing evidence for a nonequilibrium state within the surface phase. The data are used to assess existing surface rheology models.

1. Introduction

The rheological properties of fluid interfaces play a crucial role in several technological processes. Typical examples are microfluidics,[1,2] where small volumes of a liquid are manipulated, as well as all coating processes.[3] Consequently, there is a significant interest in understanding and tuning the interfacial properties of a fluid with the aid of soluble surfactants.[4,5] Their spontaneous adsorption at the air−water or oil−water interface reduces the surface tension and modifies the interfacial rheology.[6] Foams and emulsions are also partly governed by surface rheology. Several papers could successfully link the real part of the surface dilational modulus to the ability of the system to form a wet foam lamella;[7,8] furthermore, a correlation between the lifetime of a individual stable foam lamella and the imaginary part of ϵ could be established.[9,10]

The surface elastic dilational modulus ϵ is defined in analogy with the corresponding bulk quantity as the change in the surface pressure Π upon a relative area change $\Delta A/A$.[12] It is a measure for the ability of the system to adjust its surface tension in an instant of stress. The experimental determination of the dilational modulus ϵ requires the measurement of the dynamic surface tension upon harmonic compression and expansion cycles of the surface layer. The relative area change $\Delta A/A$ and the corresponding surface tension γ are the experimental quantities required for a calculation of the surface dilational module ϵ.

The surface dilational modulus is in general complex and depends on the frequency. The compression and expansion cycles of the surface layer disturb the prevailing equilibrium. As a consequence, amphiphiles must dissolve to the bulk or adsorb at the interface to restore the equilibrium coverage. It is important to compare the time frame of the internal relaxation processes with the one of the external perturbations. There is no resistance against area changes and the surface remains in equilibrium if the external frequency is on this scale small. On the other hand, at very high frequencies, the molecular exchange is suppressed and the adsorption layer behaves similar to an insoluble monolayer. The most interesting range is the intermediate mid-frequency range, which is for soluble surfactants, around 1−500 Hz.

Several arrangements have been used for the measurement of the complex ϵ modulus,[11] the classic experiment uses oscillating moving barrier devices. For technical reasons, the upper frequency limit is on the order of 0.01 Hz.[13] A larger frequency range can be covered by the excitation of surface waves and their optical evaluation.[14−20] However, the data analysis is fairly complex, and the results depend critically on the surface model. A further common alternative is oscillating drop/bubble shape tensiometry. The shape of a drop is given by the balance between gravity and surface tension. The evaluation of the drop shape according to the Gauss−Laplace equation yields the surface tension and the corresponding surface area. This measurement scheme is implemented in many commercial tensiometers; however, a careful assessment of the limitations reveals an upper physical limit of about 1 Hz, as discussed by Leser et al.[21]

Despite its obvious limitation, much work has been performed in the low-frequency range (<1 Hz),[22−28] where the equilibrium is usually established well within the time scale; consequently,

* Corresponding author. E-mail: hubert.motschmann@mpikg.mpg.de.

10.1021/jp063014l CCC: $33.50
Published on Web 08/30/2006

most of the theoretical models discussed in the literature are based on the assumption of fast equilibration. Nevertheless, these experiments revealed interesting correlations between stability of wet foams and dynamic surface elasticity[7,8] as well as dynamic shear surface moduli.[29] Thus, several groups[8,29] recognized the importance of experiments at higher frequencies.

An interesting and superior alternative to oscillating drop tensiometry is capillary pressure tensiometry.[30,31] A bubble is formed at the tip of a small capillary (diameter about 0.4 mm) and forced by a piezo translator in a well-defined oscillation. Instead of analyzing the drop shape, the pressure difference p_c across the bubble interface is measured. This arrangement allows the precise measurement of the modulus ϵ in the important mid-frequency range of 1−500 Hz, with room for improvement in both directions. The complex surface dilational modulus $\epsilon = E^* \exp^{(i\phi)}$ can be obtained by analyzing the amplitude of the pressure response and the relative phase shift between the applied sinusoidal piezo voltage and the sinusoidal pressure response. This technique has been successfully applied to several aqueous surfactant solutions.

The measurements of the surface dilational modulus of surfactant solutions in the mid-frequency range can be classified according to their behavior at higher frequencies. In the first group, the equilibrium between surface layer and bulk is instantaneously established and all dissipative losses are located within the bulk. The surface tension is then only a function of the surface composition and only the bulk diffusion causes a viscous effect at lower frequencies. The surface rheology is characterized by an increase of the monotonic amplitude E of the complex modulus to a limiting value at higher frequencies; the corresponding phase angle ϕ decreases monotonically and vanishes at higher frequencies. At higher frequencies, the surface layer behaves purely elastic. The second group of surfactants is characterized by a continuous increase of E with the frequency. The corresponding phase ϕ changes non-monotonically and does not vanish at higher frequencies. The surface layer shows a surface viscoelastic behavior at all frequencies. The differences between both types are especially pronounced at higher frequencies, whereas at lower frequencies (<100 Hz), the system response of both types are quite comparable.[5] Surface viscoelastic behavior implies that energy is dissipated not only in the bulk but also in the surface layer. It can be accounted for by the introduction of an intrinsic surface dilational viscosity κ. The interpretation of the intrinsic surface dilation viscosity is still subject to some controversy. Several conflicting models have been suggested for the underlying dissipative process such as surfactant reorientation,[32] surface compressibility,[33] or surface reaction.[34]

The aim of this paper is to assess the model for the frequency dependence of the modulus and to provide interpretative elements for the ongoing debate. In particular, we want to examine the influence of the compositional term on the surface modulus ϵ.[35,36] For such purposes, we designed an experiment where the nonequilibrium state of the surface layer can also be probed with a nonlinear optical technique, i.e., the second-harmonic generation, SHG, which is a surface specific probe. It can be used to determine the surface composition under dynamic conditions. This is required for an isolation of the impact of the compositional term to the surface dilational modulus. For clarity, we discuss briefly the background of SHG and surface rheology.

1.1. Background SHG. SHG is a nonlinear optical process based on a second-order effect.[37,38] It selectively probes interfaces because such processes are not stimulated in centrosymmetric media, at least within the framework of the electric dipole approximation. Hence, the bulk of a liquid does not contribute to the second-order nonlinear optical signal. At the surface, the inversion symmetry is broken and therefore SHG is allowed. The SHG signal is only generated within the interfacial area, and contributions arising from the bulk are suppressed.

The decisive structural information is contained in the second-order nonlinear susceptibility. In our case, SHG is determined by the dipolar contribution, and combinations of various components of the macroscopic susceptibility tensor $\chi^{(2)}$ are measured within a reflection experiment. The relation between the elements of the macroscopic susceptibility tensor $\chi^{(2)}$ and the corresponding molecular quantities is provided by the oriented gas model:[39,40]

$$\chi^{(2)} \propto \sum_{\text{mol}} \beta \propto N\langle\beta\rangle \tag{1}$$

It states that the susceptibility $\chi^{(2)}$ is the sum of the hyperpolarizabilities β of all molecules. Alternatively, this can be expressed in terms of the number density of the SHG active molecules, N, and the corresponding orientational average, $\langle\beta\rangle$, as denoted by the brackets. The orientational average is responsible for the high surface specificity of SHG experiments. In short, SHG is highly surface specific and can be used to probe the orientation and the number density of adsorbed molecules in the uppermost monolayer.

1.2. Surface Dilational Rheology. The surface elastic modulus ϵ is defined in the change in the surface pressure Π upon a relative area change $\Delta A/A$.

$$\epsilon = -\frac{\mathrm{d}\Pi}{\mathrm{d}\ln A} \tag{2}$$

We can classify the behavior of the system according to the response upon harmonic perturbations at higher frequencies in two groups: the surface elastic and surface viscoelastic behavior. In general, the surface modulus is a complex quantity characterized by its magnitude and the corresponding phase angle.

$$\epsilon(\omega, c) = E(\omega, c)\exp(i\phi(\omega, c)) \tag{3}$$

1.2.1. Surface Elastic Behavior: High-Frequency Limit. The equilibrium is instantaneously established between surface layer and bulk, and the dissipative losses are only located in the bulk. The response is fully described by the Lucassen−van den Tempel−Hansen (LvdTH) modulus,[23] which reads:

$$\epsilon'(\omega, c) = E(\omega, c)\exp(i\phi(\omega, c)) = \epsilon_m \frac{1+\zeta+i\zeta}{1+2\zeta+2\zeta^2} \tag{4}$$

with $\omega = 2\pi f$, $\omega_g(c) = D(\mathrm{d}c/\mathrm{d}\Gamma)^2$, D is the diffusion coefficient of the surfactant in the bulk, and $\zeta = \sqrt{\omega_g/2\omega}$.[5]

The derivation of eq 4 takes the equilibrium conditions at the surface into account and considers the diffusion of soluble surfactants in the adjacent bulk phase during the compression−dilation cycles. The interfacial area is divided in an uppermost monolayer and a sublayer. The concentration c_d at the boundary between subphase and bulk varies under dynamic conditions. However, it is assumed that the equilibrium at this boundary is instantaneously established, in other words, Γ depends only on the local concentration $\Gamma = \Gamma((c(t)))$. The determination of Γ requires detailed information about the structure of the surface. Γ can be calculated by an analysis of the equilibrium surface tension isotherm, provided that the effective surface layer is

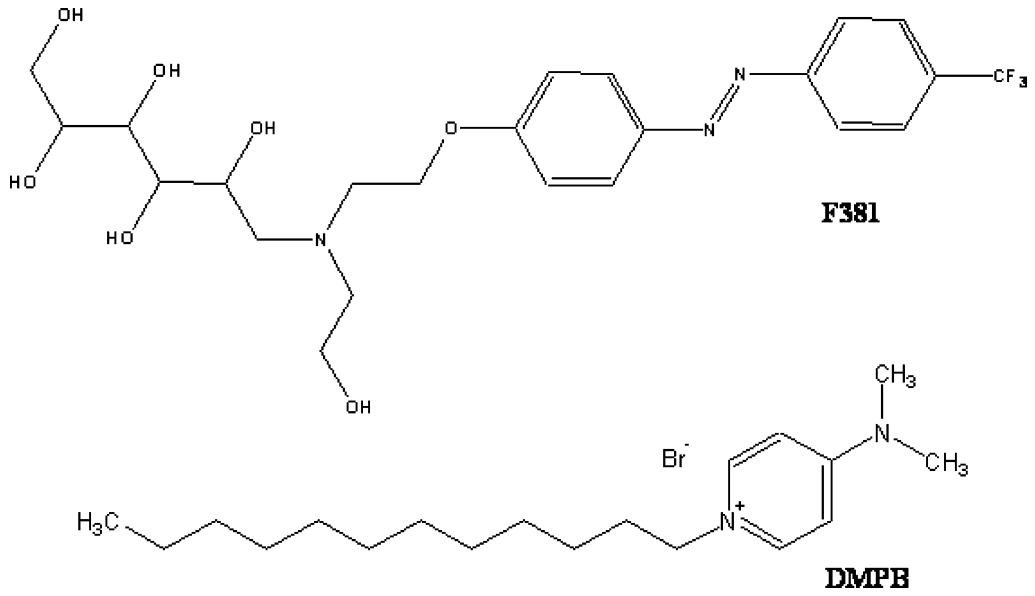

Figure 1. Chemical structures of F381 and DMPB.

only a monolayer, which means $\Gamma = \Gamma_m$. Then eq 4 yields a frequency dependence of the modulus with the following characteristics: the amplitude E is small at low frequencies ($\omega \ll \omega_g$) and increases with frequency f. At high frequencies ($\omega \gg \omega_g$), the adsorbed surfactants behave as an insoluble monolayer ($A\Gamma$ = constant), and $\epsilon(f, c)$ in eq 4 reaches a plateau value. The product of surface coverage Γ and surface area A is then constant, and furthermore, $d \ln A = -d \ln \Gamma$. In the case of a monolayer model, the measured surface dilational modulus ϵ_m in the level range should be equivalent to the Gibbs elasticity ϵ_g, which can be obtained from analysis of the equilibrium surface tension isotherm. It does not hold if the effective surface phase has an internal structure.

This model has been further extended to account for further observational facts.[41−43] From an experimental point of view, it is of utmost importance that the frequency range of the oscillation occurs in the appropriate time interval to capture the influence of the molecular exchange processes. For classical soluble surfactants, the most interesting frequency range is the range of 1−500 Hz, which is covered by our device.

1.2.2. Surface Viscoelastic Behavior: High-Frequency Limit. The most prominent feature of surface viscoelastic case is a nonvanishing phase ϕ at higher frequencies. The surface modulus remains a complex quantity at all frequencies, which can be accounted for by the introduction of an intrinsic surface dilational viscosity κ.

$$\epsilon(\omega, c) = \epsilon_g\left(\frac{1 + \zeta' + i\zeta'}{1 + 2\zeta' + 2(\zeta')^2}\right) + i\kappa\omega \qquad (5)$$

The intrinsic surface dilational viscosity κ contributes to the imaginary part of the complex module ϵ. As a consequence, the absolute value E of the modulus increases with the frequency in a monotoneous fashion. Furthermore, the function ζ of eq 4 must be replaced by the complex expression $\zeta' = h(f)\zeta$ with

$$h(\omega) = \frac{k}{(k + (1 + i)\sqrt{(\omega D/2)})} \qquad (6)$$

that characterizes the nonequilibrium state within the surface layer. The kinetically controlled surfactant exchange is captured by the rate constant k. If the rate constant is big ($k^2 \gg \omega D$), the molecular exchange between monolayer and sublayer is sufficiently fast that the equilibrium state within the surface layer is instantaneously established and h becomes 1.[30,35,44] The rate constant k is an important fitting parameter obtained by an analysis of the frequency dependence of the complex module.

2. Experimental Section

2.1. Materials. A fluoroazobenzene-based surfactant, F381, and a cationic surfactant, dodecyl-dimethylaminopyridinium bromide, DMPB, are depicted in Figure 1. The surfactants were purified prior to usage. Details on the synthesis can be found in ref 45. In order to fully utilize the potential of SHG, a hyperpolarisibility is required. This is achieved by the electronic π system of the headgroup with a donor or and an acceptor group. The design of our model systems takes this into consideration.

2.2. Surface Rheological Measurements: Oscillating Bubble Technique. The principle of the oscillating bubble technique is sketched in Figure 2 showing a cross-sectional view of the chamber.

A small hemispherical bubble is formed at the tip of a capillary with a radius of about 0.2 mm. The bubble is forced in a sinusoidal oscillation by a piezoelectric translator which is directly immersed in the liquid. As a result, a harmonic modulation of the pressure in the chamber is observed and recorded by a sensitive pressure transducer located at the bottom of the chamber.

The amplitude of the pressure response and the phase shift between piezo oscillation and pressure signal are determined by a phase-sensitive lock-in detector. The amplitude of the pressure response is proportional to that of the complex surface dilational modulus E, while the phase shift yields the imaginary part of the modulus, in other words, the surface dilational viscosity.

2.3. Oscillating Bubble Technique Combined to SHG. The oscillating bubble technique forces the surface layer in a nonequilibrium state. The pressure sensor measures the complex surface dilational elasticity module while second-harmonic generation (SHG) allows the determination of the surface coverage within the topmost monolayer under dynamic conditions. The experimental arrangement is shown in Figure 2. SHG experiments require high-energy laser pulses in order to generate the high electromagnetic fields that are a prerequisite of

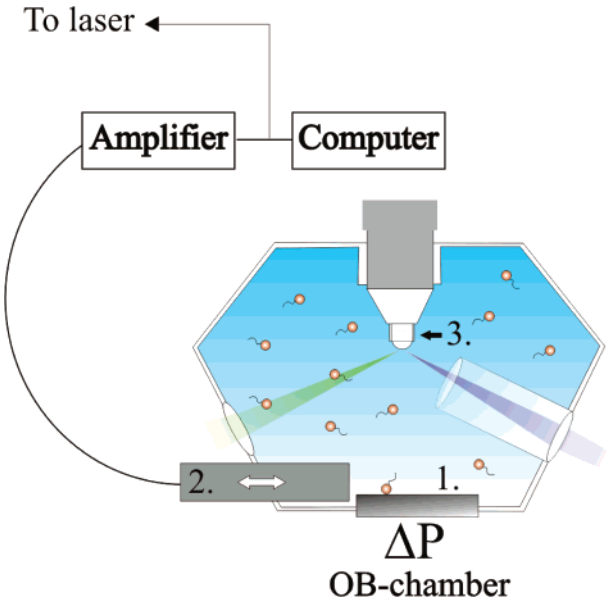

Figure 2. Cross-sectional view of the oscillating bubble device. The piezo translator is immersed in the liquid, the bubble is formed at the tip of the capillary, and the pressure is recorded by a sensitive pressure transducer at the bottom of the chamber. The piezo movement leads to an expansion and compression of the surface layer. The surface state can also be probed by second-harmonic generation in total reflection mode. The bubble oscillation is then synchronized with the laser system.

detectable nonlinear optical effects. The laser pulses have to be synchronized with the bubble oscillations so that the fluid surface of the bubble can be probed during the oscillation cycle. The instrumentation is described in detail by Örtegren et al.[46] Measurements with the surfactant F381 were performed with the frequency-doubled light at 532 nm of the Nd:YAG laser. The laser energy was about 35 mJ per pulse.

The experiments with the viscoelastic compound, DMPB, required some modifications of the original setup. To overcome the UV absorption within the solutions in the chamber, a UV-transparent cuvette has been mounted on the exit side of the chamber in close proximity to the capillary. Second, we used laser pulses at 650 nm for the SHG experiments, which were generated by pumping an optical parametric generator/amplifier with the tripled (355 nm) Nd:YAG line. The weak signal due to the smaller hyperpolarizibility of this molecule could be compensated by the resonance enhancement. The laser energy was about 0.15 mJ per pulse. The plane of polarization of the light probing the tip of the bubble was rotated 39° from vertical polarization, where the SHG apparent molecular tilt angle is fairly independent of the true distribution mean.[47] Spectral purity of the incoming and detected light was assured by the use of filters.

At least 10 measurements were performed at each phase angle, and each measurement is the average of the intensity of 100−200 laser pulses of SHG light reflected at the bubble surface. Each measurement on the tip of the bubble in DMPB solutions was done on a freshly formed surface because the pump light leads to some photo bleaching of the surfactant. The SHG signal from pure water was used as background and subtracted from the presented data. It is important to note that different capillary sizes have to be used for oscillating bubble tensiometry and the SHG combined to oscillating bubble, SHG-OB, experiment. As a consequence, the higher frequency limit reached by the systems differ; for the oscillating bubble tensiometry, it is possible to reach 500 Hz as a limit, whereas for the SHG-OB, the upper limit is about 60 Hz.

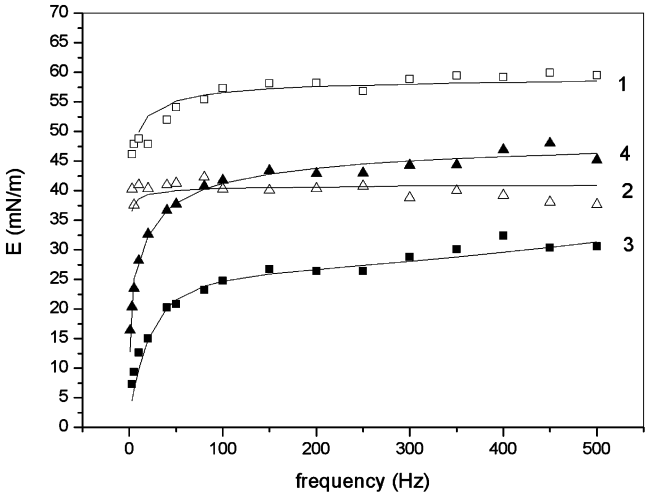

Figure 3. Absolute value E of surface elasticity modulus ϵ measured by oscillating bubble tensiometry as a function of frequency: The solid line represents the theory, the open squares refer to a concentration of 0.150 mM of the surfactant F381 (curve 1), the open triangles to 0.030 mM of the surfactant F381 (curve 2), the solid squares to 4 mM DMPB (curve 3), and the solid triangles to a 1 mM DMPB solution (curve 4).

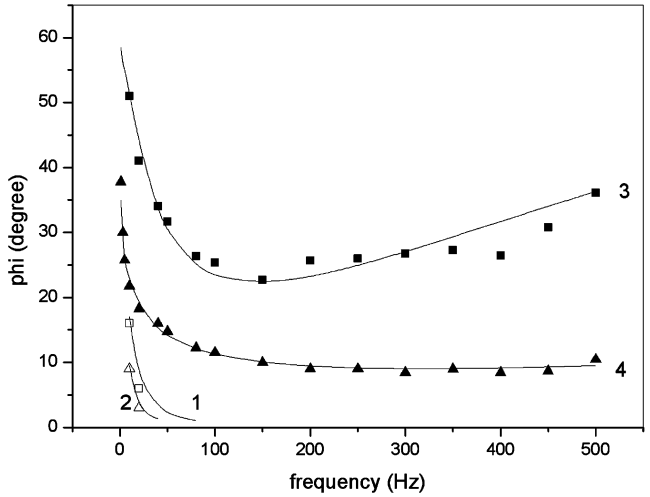

Figure 4. Phase angle of surface elasticity modulus measured by oscillating bubble tensiometry as a function of oscillation frequency: The solid line represents the theory, the open squares refer to a concentration of 0.150 mM of the surfactant F381 (curve 1), the open triangles to 0.030 mM of the surfactant F381 (curve 2), the solid squares to 4 mM DMPB (curve 3), and the solid triangles to a 1 mM DMPB solution (curve 4).

3. Results and Discussion

3.1. Tensiometric Studies in the Oscillating Bubble Configuration. The frequency dependence of the amplitude E of the modulus ϵ of the surfactant for DMPB is shown in Figure 3. The system shows at low concentrations an elastic behavior. However, at higher concentrations (>0.5 mM), a crossover to surface viscoelastic behavior is observed. The absolute value E is plotted for two different concentrations of DMPB (4 mM, curve 3, and 1 mM, curve 4). The absolute value of E increases in a monotoneous fashion. The corresponding phase measurement is shown in Figure 4. At higher frequencies, there is a nonvanishing phase, and the system behaves viscoelastically at all frequencies. The surfactant F381 is discussed in ref 49. The system behaves purely elastically at all concentrations and can serve as a model system for the surface elastic behavior. We use these data for comparison purposes with the viscoelastic model. Figures 3 and 4 contain the absolute value E and the

phase for the surfactant F381. The limiting value of E is reached at frequencies exceeding 20 Hz. The corresponding phase vanishes then. Curve 1 refers to a concentration of F381 0.15 mM, curve 2 to a surfactant concentration of 0.03 mM.

3.2. SHG Studies in the Oscillating Bubble Configuration for an Elastic Model System. The SHG experiments allow the independent assessment of the surface models describing the frequency dependence of the modulus. The ϵ modulus obtained with the oscillating bubble tensiometry can be directly compared with the relation of the monolayer concentration Γ_m, which are obtained by the SHG measurements:

$$\Delta\gamma = \epsilon(\omega, c)\frac{\Delta A}{A} = E(\omega, c)\exp(i(\phi(\omega, c)))\frac{\Delta A}{A} \quad (7)$$

$$\frac{\Delta\Gamma_m(\omega, c)}{\Gamma_m} = |\Delta\Gamma^*(\omega, c)|\exp(i(\alpha(\omega, c)))\frac{-\Delta A}{A} \quad (8)$$

It is desirable to introduce the following real quantities, which are all experimentally accessible: The normalized area change

$$\Delta A^*(\psi) = \frac{\Delta A}{|A|} = -\sin\psi \quad (9)$$

The normalized change in monolayer concentration

$$\Delta\Gamma^*(\psi) = \left|\frac{A}{\Delta A}\right|\frac{\Delta\Gamma_{SHG}}{\Gamma_{SHG}} = \left|\frac{A}{\Delta A}\right|\cdot\frac{(\Gamma_{SHG(\Psi)} - \bar{\Gamma}_{SHG})}{\bar{\Gamma}_{SHG}} \quad (10)$$

normalized change in dynamic surface tension.

$$\Delta\gamma^*(\psi) = |\epsilon(\omega)/\epsilon_m|\sin(\psi - \phi) \quad (11)$$

The quantity $\psi = \omega\cdot t\cdot 360°/2\pi$ represents the phase of the area change, $\Gamma_{SHG}(\psi)$ the surface coverage measured under dynamic conditions by SHG, and $\bar{\Gamma}_{SHG}$ the mean of the monolayer concentration.

The quantities ΔA^*, $\Delta\Gamma^*$, and $\Delta\gamma^*$ have been determined for the model component F381 as a function of the angle ψ at oscillation frequency of $f = 40$ Hz. It turned out that the change in area in monolayer concentration determined with the SHG and in dynamic surface tension are in phase for all concentrations. A further interesting feature is a decrease of the monolayer concentration $\Delta\Gamma^*$ under dynamic conditions with a increase of the bulk concentration. A value of $\Delta\Gamma^* = 0.97$ was determined at a concentration of 10 mM, whereas a value of $\Delta\Gamma^* = 0.45$ was determined for a 110 mM solution of F381 in water. In these experiments, the influence of the bulk diffusion is negligible, as indicated by the vanishing phase angle. That means the relation

$$\frac{\Delta\Gamma}{\Gamma} = -\frac{\Delta A}{A} \quad (12)$$

is valid. The normalized amplitude $\Delta\Gamma^*$ shows that, for low concentrations, only the monolayer represents the effective surface layer because eq 8 can be replaced by, according to the SHG experiments:

$$\frac{\Delta\Gamma_m}{\Gamma_m} = -\frac{\Delta A}{A} \quad (13)$$

However, for higher concentrations becomes

$$\left|\frac{\Delta\Gamma_m}{\Gamma_m}\right| < \left|\frac{\Delta A}{A}\right| \quad (14)$$

Therefore, a sublayer is enriched with surfactant and a molecular exchange between this sublayer and the monolayer must be introduced in order to fulfill eq 12.

This model can be explained by using another argument, too. In the equilibrium state of the surface layer, the net flux j between monolayer and sublayer becomes zero and the isotherm equation $\gamma = \gamma(\Gamma_m(c_d))$ is fulfilled (c_d concentration at the boundary of the bulk phase and the interfacial region which can be artificially fixed). This condition is also fulfilled during an expansion or compression of the surface if the molecular exchange processes within the surface layer and between the surface layer and uppermost layer of the bulk are sufficiently fast that the equilibrium is instantaneously established. Then the change in the surface area causes only a bulk diffusion, which leads to the LvdTH modulus.

The periodic expansion compression cycles lead to an oscillating solution of the diffusion equation, x is the coordinate perpendicular to the surface, $k' = \sqrt{\omega/D}$ refers to the wavenumber of the diffusion wave, and β^* denotes the corresponding phase angle.

$$\Delta c(x, t) = c(x, t) - c_0 = |\Delta c_d|\exp((1 + i)k'x - i\omega t + i\beta^*) \quad (15)$$

The expression yields at $x = -d$ a molecular exchange rate of

$$\frac{\Gamma}{A}\frac{dA(t)}{dt} + \frac{d\Gamma}{dt} = -D\frac{\partial c}{\partial x}\Big|_{x=-d} = -(1 + i)\sqrt{\frac{\omega D}{2}}\frac{dc_d}{d\Gamma}\Delta\Gamma = -(1 + i)\sqrt{\frac{\omega\omega_m}{2}}\Delta\Gamma \quad (16)$$

This ansatz leads to eq 4, which represents a subset of the more general eq 5. It is important to stress that the final equations are independent of the layer thickness. The relevant parameters are obtained by a least-squares fitting procedure. According to eq 16, ω_m determines the molecular exchange between the interface of bulk and surface phase. Time integration and arithmetic rearrangement of eq 16 yields

$$\frac{\Delta A}{A} = \left((-1 + i)\sqrt{\frac{\omega_m}{2\omega}} - 1\right)\frac{\Delta\Gamma}{\Gamma} \quad (17)$$

for the relation between the relative change in the surface area and the relative change in the surface concentration if bulk diffusion takes place. At higher frequencies $\omega \gg \omega_m$, eq 17 simplifies to eq 12.

In the plateau range of this modulus characterized by the condition $\omega_m \ll \omega$, the molecular exchange can be neglected due to the small disturbance of the concentration in the bulk by the surface deformation. This is the reason for the quasi-insoluble behavior in level range of the LvdTH model, although there, the equilibrium condition is not violated. With eq 12 and $\omega_m(c) = D(dc/d\Gamma)^2$, it follows for the disturbance of the concentration in the topmost layer of the bulk

$$\Delta c = \sqrt{\omega_m/D}\Delta\Gamma = -\sqrt{\omega_m/D}\Gamma\Delta A/A \quad (18)$$

The inequality $\omega_m < \omega_g$ means that the real disturbance of the bulk concentration is smaller than the disturbance calculated with the aim of the isotherm. This is possible if the sublayer

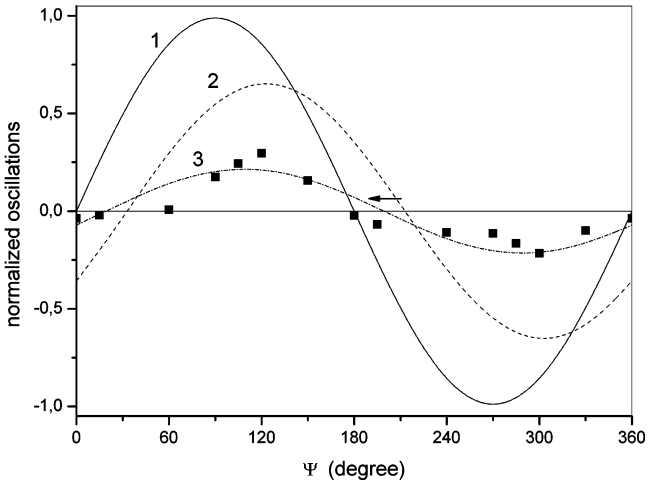

Figure 5. Dynamic characteristics of surfaces of 4 mM DMPB solutions as function of the phase angle $\Psi = (t/0.025\ \text{s})\cdot 360°$, $f = 40$ Hz. The solid line represents the normalized area change $\Delta A^* = -\sin \Psi$, the dashed line represents the normalized change in dynamic surface tension $\Delta\gamma^* = |\epsilon(f)/\epsilon_m| \sin(\Psi - \phi)$, the square dots are the changes in the surface coverage $\Delta\Gamma$. The solid line represents the basic Fourier component.

possesses an enriched concentration in comparison to the bulk concentration. A similar argument can be made for the differences of the Gibbs elasticity ϵ_g and the high-frequency limit ϵ_m of the oscillating bubble measurement. From the approximation

$$\epsilon_m = -\frac{\Delta\gamma}{\Delta \ln \Gamma_m}\frac{\Delta\Gamma_m}{\Gamma_m}\frac{\Gamma}{\Delta\Gamma} \approx \epsilon_g \frac{\Delta\Gamma_m}{\Gamma_m}\frac{\Gamma}{\Delta\Gamma} \tag{19}$$

follows for $\epsilon_m < \epsilon_g$ the inequality

$$\left|\frac{\Delta\Gamma_m}{\Gamma_m}\right| < \left|\frac{\Delta\Gamma}{\Gamma}\right| = \left|\frac{\Delta A}{A}\right| \tag{20}$$

As mentioned above, this can be interpreted as a consequence of the molecular exchange between the monolayer and an enriched sublayer, neglecting the exchange with the bulk, which is characteristic of the plateau range at higher frequencies. The SHG experiments with F381 solutions lend support to this interpretation.

3.3. SHG Studies in the Oscillating Bubble Configuration for a Viscoelastic Model System. The SHG experiment on DMPB are much more demanding due to the low hyperpolarizability of the molecule. The experiments required the utilization of resonance enhancement using a rather complex laser system. Laser pulses at a wavelength of 650 nm have been generated by an optical parametric amplifier and generator. Figure 5 shows the data ΔA^*, $\Delta\Gamma^*$, and $\Delta\gamma^*$of a 4 mM DMPB solutions.

The data show a a phase shift between the maximum compression and the maximum signal measured. Moreover, the relative magnitude of the measured concentration of surfactants in the monolayer during oscillation, calculated from the experimental data, is $\Delta\Gamma/\Gamma_{SHG} = 0.063$ in the case of 1 mM and 0.05 for the 4 mM solution. We observe that, in both cases, $\Delta\Gamma_m/\Gamma_m \approx \Delta\Gamma_{SHG}/\Gamma_{SHG}$ is smaller than the relative magnitude of the surface area (0.18 ± 0.04). Finally, the relative change of the concentration of surfactants in the monolayer decreases with the concentration.

The DMPB solutions exhibited surface viscoelastic behavior at all frequencies, as revealed in Figures 3 and 4. In the case of viscoelastic response, it must be as well $\alpha(f, c) \neq 0$ as $\phi(f, c) \neq 0$. The phase angle $\alpha(f, c)$ is caused by the bulk diffusion and $h(f)$, whereas $\phi(f, c)$ is influenced by the intrinsic dilational viscosity via $i\omega\kappa$. In the equilibrium state, it becomes $h(f) = 1$ and $\kappa \approx 0$. Then, $\epsilon(f, c)$ can be approximated by the LvdTH modulus, whereas experimental results with

TABLE 1

compd	c M [mmol]	ϵ_m mN/m	ω_m s^{-1}	κ mNs/m	$\approx k$ cm s^{-1}	$\approx I$ mol cm s^{-1}
DMPB	1	48.1	58	0.0013	0.22	0.22×10^{-6}
DMPB	4	26.8	570	0.005	0.33	0.13×10^{-6}

$$\alpha(f, c) \neq \phi(f, c) \tag{21}$$

indicate a nonequilibrium state in the surface layer and the influence of the intrinsic surface dilational viscosity κ on the dynamic surface tension. Consequently, only the complete eq 5 describes correctly the modulus $\epsilon(f, c)$. In addition, the following relation must hold $\alpha(f, c) < \phi(f, c)$ because $\alpha(f, c)$ represents the directly measured phase angle of the $\Delta\Gamma_m$, which should be equal to the phase angle of the first term of eq 5 or the LvdTH modulus due to the eq 4, whereas the term $i\omega\kappa$ increases the phase angle in eq 5.

The adsorption layer of the cationic surfactant DMPB behaves viscoelastically in the low and the higher frequency range. Hence, we must must consider bulk diffusion and the intrinsic surface viscosity, as given by eq 5. Table 1 lists the results of a least-squares fit. The magnitude of the molecular exchange rate constant k suggests a nonequilibrium state between the monolayer and sublayer in the entire frequency range. This supports the hypothesis that the intrinsic surface dilational viscosity is caused by the molecular exchange between structural elements that are not in equilibrium. The SHG measurements supports this model. The Fourier analysis of $\Delta\Gamma^*$ leads to the inequality $\alpha(f, c) < \phi(f, c)$ for the basic oscillation. This provides corroborative evidence that the intrinsic surface viscosity is the result of a nonequilibrium state between monolayer and sublayer. However, the higher harmonic components are too big for a quantitative assessment. A surface viscosity of $\kappa = 0.005$ mNs/m (see Table 1) leads to a difference of 4° between $\phi(f, c)$ ($f = 40$ Hz, $c = 4$ mM) and α ($f = 40$ Hz, $c = 4$ mM). The error of the measurements of both phase angles is on the same order so that only the inequality $\alpha(f, c) < \phi(f, c)$ can be verified by the SHG measurements. Unfortunately, the present experimental instrumentation imposes an upper limit around 60 Hz; hence, it is not yet possible to perform SHG measurements at the higher frequency range where the intrinsic viscous effect is dominant.

The amplitude of $\Delta\Gamma^*$ is clearly smaller than one and also smaller than $\Delta\gamma^*$. For the interpretation of these effects, we must take into account that an ionic surfactant in all cases forms a sublayer with an internal structure, which in turn must have influence on the surface tension. Consequently, "enriched" means a higher neutral sublayer concentration, which has to be accounted for when solving the Laplace−Boltzmann equation. The thickness of the sublayer is smaller than 10 nm, as SAXS measurements performed on a nonionic surfactant demonstrate (unpublished results). This means that energy states of the molecules deviate only in a layer of a few nm from their energy states within the bulk far from the surface. This layer is smaller than the Debye length of a 1 mM solution of an ionic surfactant, about 10 nm. At present, the database is too small to deduce a detailed quantitative model. The amplitude of the normalized dynamic surface tension $\Delta\gamma^*$ exceeds the amplitude of the normalized monolayer concentration $\Delta\Gamma^*$, which supports our

interpretation. The SHG measurements provide corroborative evidence for several critical aspects of surface rheology.

4. Conclusion

Oscillating bubble second-harmonic generation (SHG) measurements were performed in the medium-frequency range on a surface elastic system and a surface viscoelastic system. The optical setup allows the direct measurements of the concentration of soluble surfactants in the monolayer Γ_m under dynamic conditions. The measurements on the elastic system solutions were done at frequencies where the influence of the bulk diffusion is negligible. It was found that, for low concentrations, the relative change in the monolayer concentration Γ_m during oscillation, $\Delta\Gamma_m$, was equal to the negative relative change in surface area during oscillation, $-\Delta A/A$, whereas at higher concentrations, both solutions show a distinct reduction of $\Delta\Gamma_m/\Gamma_m$. For F381 solutions, the oscillations of $\Delta\Gamma_m$ and $\Delta A/A$ are in phase, while DMPB shows a phase shift of $\Delta\Gamma_m/\Gamma_m$. The comparison of this phase angle with the phase of the surface dilational modulus exhibit the influence of the bulk diffusion and the intrinsic surface dilational viscosity.

The data can be explained by a molecular exchange process described by a modified Lucassen−van den Tempel−Hansen model, in which the surface is assumed to consist of a monolayer and an adjacent sublayer. If the molecular exchange between both structures is fast enough, then the surface response is elastic provided that the diffusion is negligible. This could be demonstrated by measurements of the surface dilational moduli with F381 solutions and verified by SHG measurements. For lower molecular exchange rates, an expansion or compression of the surface leads to a nonequilibrium state between the internal structures of the surface layer. Then, the molecular exchanges can cause a dissipative loss and an intrinsic viscous effect. The surface dilatational modulus of DMPB solutions show such behavior. The SHG measurements provide corroborative evidence for a nonequilibrium state within the surface and help to clarify critical issues of surface rheology.

Acknowledgment. We gratefully acknowledge financial support from the Max-Planck-Gesellschaft and the Deutsche Forschungsgemeinschaft. We are grateful for Prof. Möhwald continuous support and stimulating discussions. Furthermore, we thank our laboratory technicians G. Wienskol and I. Bartsch as well as C. Stolle for the synthesis of the surfactants.

References and Notes

(1) Koester, S.; Steinhauser, D.; Pfohl, T. *J. Phys., Condens. Matter* **2005**, *17*, S4091.
(2) Otten, A.; Köster, S.; Struth, B.; Snigirev, ; Pfohl, Th. *J. Synchrotron Radiat.* **2005**, *12*, 745.
(3) Ascanio, G.; Carreau, P. J.; Tanguy, P. A. *Exp. Fluids* **2006**, *40*, 1.
(4) Dukhin, S. S., Kretzschmar, G., Miller, R., Eds. *Dynamics of Adsorption at Liquid Interfaces*; Studies in Interface Science Series; Elsevier: Amsterdam, 1995; p 1.
(5) Möbius, D., Miller, R., Eds. *Drops and Bubbles in Interfacial Research*; Studies in Interface Science Series; Elsevier: Amsterdam, 1998; p 6.
(6) Adamson, A. W.; Gast, A. P. *Physical Chemistry of Surfaces*; Wiley: New York, 1997.
(7) Wantke, K.-D.; Malysa, K.; Lunkenheimer, K. *Colloids Surf., A* **1994**, *82*, 183.
(8) Stubenrauch, C.; Miller, R. *J. Phys. Chem. B* **2004**, *108*, 6412.
(9) Fruhner, H.; Wantke, K.-D.; Lunkenheimer, K. *Colloids Surf., A* **1999**, *162*, 193.
(10) Koelsch, P.; Motschmann, H. *Langmuir* **2005**, *21*, 6265.
(11) Miller, R.; Fainerman, V. B.; Makievski, A. V.; Ferrari, M.; Loglio, G. In *Handbook of Applied Surface and Colloid Chemistry*; Holmberg, K., Ed.; John Wiley & Sons: West Sussex, England, 2002; p 2.
(12) Langevin, D. *Adv. Colloid Interface Sci.* **2000**, *88*, 209.
(13) Kretschmar, G.; Li, J.; Miller, R.; Motschmann, H.; Möhwald, H. *Colloids Surf., A* **1996** *114*, 277.
(14) Bhattacharyya, A.; Monroy, F.; Langevin, D.; Argillier, J.-F. *Langmuir* **2000**, *16*, 8727.
(15) Stenvot, C.; Langevin, D. *Langmuir* **1988**, *4*, 1179.
(16) Jiang, Q.; Chiew, Y. C.; Valentini, J. E. *Langmuir* **1992**, *8*, 2747.
(17) Jiang, Q.; Chiew, Y. C.; Valentini, J. E. *J. Colloid Interface Sci.* **1993**, *155*, 8.
(18) Jayalakshmi, Y.; Ozanne, L.; Langevin, D. *J. Colloid Interface Sci.* **1995**, *170*, 358.
(19) Jayalakshmi, Y.; Langevin, D. *J. Colloid Interface Sci.* **1996**, *194*, 22.
(20) Noskov, B. A.; Grigoriev, O. G.; Miller, R. *J. Colloid Interface Sci.* **1997**, *188*, 9.
(21) Leser, M. E.; Acquistapace, S.; Cagna, S.; Makievski, A.; Miller, R. *Colloids Surf., A* **2005**, *261*, 25.
(22) Pugh, R. J. *Adv. Colloid Interface Sci.* **1996**, *64*, 67.
(23) Lucassen, J.; Van den Tempel, M. *Chem. Eng. Sci.* **1972**, *27*, 1283.
(24) Bonfillon, A.; Langevin, D. *Langmuir* **1993**, *9*, 2172.
(25) Johnson, D. O.; Stebe, K. J. *J. Colloid Interface Sci.* **1996**, *182*, 526.
(26) Noskov, B. A.; Alexandrov, D. A.; Miller, R. *J. Colloid Interface Sci.* **1999**, *219*, 250.
(27) Noskov, B. A.; Akentiev, A. V.; Bilibin, A. Y.; Zorin, I. M.; Miller, R. *Adv. Colloid Interface Sci.* **2003**, *104*, 245.
(28) Ritacco, H.; Kurlat, D.; Langevin, D. *J. Phys. Chem. B* **2003**, *107*, 9146.
(29) Monteux, C.; Fuller, G. C.; Bergeron, V. *J. Phys. Chem. B* **2004**, *108*, 16473.
(30) Fruhner, H.;Wantke, K.-D. *Colloids Surf., A* **1996**, *114*, 53.
(31) Liggieri, L.; Attolini, V.; Ferrari, M.; Ravera, F. *J. Colloid Interface Sci.* **2002**, *255*, 225.
(32) Fainerman, V. B.; Zholob, S. A.; Lucassen-Reynders, E. H.; Miller, R. *J. Colloid Interface Sci.* **2003**, *261*, 180.
(33) Fainerman, V. B.; Kovalchuk, V. I.; Leser, M. E.; Miller, R.; E*ffect of the Intrinsic Compressibility on the Dilational Rheology of Adsorption Layers of Surfactants, Proteins and Their Mixtures*; Tadros, Th., Ed.; John Wiley: New York, 2006.
(34) Ivanov, I. B.; Danov, K. D.; Ananthapadmanabhan, K. P.; Lips, A. *Adv. Colloid Interface Sci.* **2005**, *114*, 61.
(35) Wantke, K.-D.; Fruhner, K.-D. *Colloid Interface Sci.* **2001**, *237*, 185.
(36) Wantke, K.-D.; Fruhner, H.; Örtegren, J. *Colloids Surf., A* **2003**, *221*, 185.
(37) Shen, Y. R. *The Principles of Nonlinear Optics*; Wiley: New York, 1984.
(38) Eisenthal, K. B. *Chem. Rev.* **1996**, *96*, 1343.
(39) Prasad, P. N.; Williams, D. J. *Introduction to Nonlinear Optical Effects in Molecules and Polymers*; John Wiley & Sons, Inc.: New York, 1991; p 320.
(40) Motschmann, H.; Penner, T.; Armstrong, N.; Enzenyilimba, M. *J. Phys. Chem.* **1993**, *97*, 3933.
(41) Lucassen, J.; Hansen, R. *J. Colloid Interface Sci.* **1967**, *23*, 319.
(42) Lucassen, J.; van den Tempel, M. *J. Colloid Interface Sci.* **1972**, *41*, 491.
(43) Wantke, K. D.; Ortegren, J.; Fruhner, H.; Andersen, A.; Motschmann, H. *Colloids Surf., A* **2005**, *261*, 75.
(44) Wantke, K.-D.; Fruhner, H.; Fang, J.; Lunkenheimer, K. *J. Colloid Interface Sci.* **1998**, *208*, 34.
(45) Haage, K.; Motschmann, H.; Bae, S.; Gründemann, E. *Colloids Surf., A* **2001**, *183*, 583.
(46) Örtegren, J.; Wantke, K.-D.; Motschmann, H. *Rev. Sci. Instrum.* **2003**, *74*, 5167.
(47) Simpson, G. J.; Rowlen, K. L. *J. Am. Chem. Soc.* **1999**, *121*, 2635.
(48) Sohl, C. H.; Miyano, K.; Ketterson, J. B. *Rev. Sci. Instrum.* **1978**, *49*, 1464.
(49) Örtegren, J.; Wantke, K.-D.; Motschmann, H.; Möhwald, H. *J. Colloid Interface Sci.* **2004**, *279*, 266.